

$(\text{CH}_3)\text{C}(=\text{O})\text{CH}_2^*$ radical as well as the accompanying HO^* radical was formed in the O_3 -TME system via reaction 5.

To further examine the oxidation of $\text{CH}_3\text{C}(=\text{O})\text{CH}_2^*$ radicals, the photolysis of mixtures containing parts-per-million concentrations of Cl_2 and $(\text{CH}_3)_2\text{C}=\text{O}$ in air yielded methylglyoxal $\text{H}_3\text{C}(=\text{O})\text{CHO}$ as a major product, i.e., ca. 30% of $\Delta[(\text{CH}_3)_2\text{C}=\text{O}]$, which can be attributed to the oxidation of the $\text{CH}_3\text{C}(=\text{O})\text{CH}_2^*$ radical. Thus, the observation of $\text{CH}_3\text{C}(=\text{O})\text{CHO}$ in the O_3 -TME- O_2 system (cf. Tables I and II) is consistent with the formation of this radical via reaction 5. A plausible mechanism for the formation of $\text{CH}_3\text{C}(=\text{O})\text{CHO}$ is $\text{CH}_3\text{C}(=\text{O})\text{CH}_2^* + \text{O}_2 \rightarrow \text{CH}_3\text{C}(=\text{O})\text{CH}_2\text{OO}^*$; $2\text{CH}_3\text{C}(=\text{O})\text{CH}_2\text{OO}^* \rightarrow 2\text{CH}_3\text{C}(=\text{O})\text{CH}_2\text{O}^* + \text{O}_2$; and $\text{CH}_3\text{C}(=\text{O})\text{CH}_2\text{O}^* + \text{O}_2 \rightarrow \text{CH}_3\text{C}(=\text{O})\text{CHO} + \text{HOO}^*$. Under atmospheric conditions, $\text{CH}_3\text{C}(=\text{O})\text{CH}_2\text{O}^*$ may react predominantly with O_2 rather than undergoing unimolecular dissociation to CH_3CO^* and HCHO .¹² No further quantitative determination of these competing reactions was pursued in the present study. Instead, attention was focused on the detection of a carbonyl product arising from the reaction $\text{CH}_3\text{C}(=\text{O})\text{CH}_2\text{OO}^* + \text{HOO}^* \rightarrow \text{CH}_3\text{C}(=\text{O})\text{CH}_2\text{OOH} + \text{O}_2$, since this compound was suspected to be the unidentified species exhibiting the $\text{C}=\text{O}$ band at ca. 1740 cm^{-1} in the O_3 -TME reaction (cf. Figure 2C). A broad band in this frequency region could be observed in the product spectra from the photolysis of Cl_2 - $(\text{CH}_3)_2\text{C}=\text{O}$ - O_2 mixtures, but the signal/noise ratio was too poor for reliable spectral characterization. However, upon substitution with MEK which reacted much more rapidly with Cl atoms, a strong $\text{C}=\text{O}$ band centered at 1736 cm^{-1} and a weak $\text{O}-\text{H}$ band at ca. 3600 cm^{-1} most likely due to the formation of $\text{CH}_3\text{C}(=\text{O})\text{CH}(\text{CH}_3)\text{OOH}$ were readily discernible.²⁶ It was also noted in this photochemical system that the corresponding dicarbonyl $\text{CH}_3\text{C}(=\text{O})\text{C}(=\text{O})\text{CH}_3$ was observed as a major product. However, additional experiments have shown that the mechanism for the dicarbonyl formation is distinct from that in the $(\text{CH}_3)_2\text{C}=\text{O}$ system.²⁶ Namely, the overall reaction can be represented by $\text{CH}_3\text{C}(=\text{O})\text{CH}(\text{CH}_3)\text{OO}^* + \text{HOO}^* \rightarrow \text{CH}_3\text{C}(=\text{O})\text{C}(=\text{O})\text{CH}_3 + \text{H}_2\text{O} + \text{O}_2$ rather than $\text{CH}_3\text{C}(=\text{O})\text{CH}(\text{CH}_3)\text{O}^* + \text{O}_2 \rightarrow \text{CH}_3\text{C}(=\text{O})\text{C}(=\text{O})\text{CH}_3 + \text{H}_2\text{O} + \text{O}_2$.

(26) To be described in more detail elsewhere.

$\text{O})\text{CH}(\text{CH}_3)\text{O}^* + \text{O}_2 \rightarrow \text{CH}_3\text{C}(=\text{O})\text{C}(=\text{O})\text{CH}_3 + \text{HOO}^*$. Although it has not been established whether this novel reaction occurs entirely in the gas phase or involves heterogeneous processes, e.g., $\text{CH}_3\text{C}(=\text{O})\text{CH}(\text{CH}_3)\text{OOH} (+ \text{wall}) \rightarrow \text{CH}_3\text{C}(=\text{O})\text{C}(=\text{O})\text{CH}_3 + \text{H}_2\text{O}$, an analogous reaction may account, in part, for the observation of $\text{CH}_3\text{C}(=\text{O})\text{CHO}$ in the photolysis of Cl_2 - $(\text{CH}_3)_2\text{C}=\text{O}$ -air and in the O_3 -TME-air system.

Further corroborative evidence for the occurrence of the reaction of HO^* with TME in the O_3 -TME-air system was obtained by a product study in the photolysis of mixtures containing parts-per-million concentrations of CH_3ONO , NO , and TME in air.²⁶ In these mixtures, the HO^* radicals are generated photochemically via the series of reactions: $\text{CH}_3\text{ONO} + h\nu (>300\text{ nm}) \rightarrow \text{CH}_3\text{O}^* + \text{NO}$; $\text{CH}_3\text{O}^* + \text{O}_2 \rightarrow \text{HCHO} + \text{HOO}^*$; and $\text{HOO}^* + \text{NO} \rightarrow \text{HO}^* + \text{NO}_2$.^{12,13} Acetone was the predominant C-containing product with its yield $\Delta[(\text{CH}_3)_2\text{C}=\text{O}]/\Delta[\text{TME}] = 1.7 \pm 0.1$ and the remainder as an unidentified organic nitrate. These results suggest that the NO reaction of the peroxy radical $(\text{CH}_3)_2\text{C}(\text{OH})\text{C}(\text{CH}_3)_2\text{OO}^*$ formed by the successive addition of HO^* and O_2 to TME yielded $(\text{CH}_3)_2\text{C}(\text{OH})\text{C}(\text{CH}_3)_2\text{O}^*$ (85%) and $(\text{C}-\text{H}_3)_2\text{C}(\text{OH})\text{C}(\text{CH}_3)_2\text{ONO}_2$ (15%) and that $(\text{CH}_3)_2\text{C}(\text{OH})\text{C}(\text{CH}_3)_2\text{O}^*$ was converted to $(\text{CH}_3)_2\text{C}=\text{O}$ via $(\text{CH}_3)_2\text{C}(\text{OH})\text{C}(\text{CH}_3)_2\text{O}^* \rightarrow (\text{CH}_3)_2\text{C}(\text{OH})^* + (\text{CH}_3)_2\text{C}=\text{O}$ followed by $(\text{CH}_3)_2\text{C}(\text{OH})^* + \text{O}_2 \rightarrow (\text{CH}_3)_2\text{C}=\text{O} + \text{HOO}^*$.¹² Thus, in the O_3 -TME-air system, the excess $(\text{CH}_3)_2\text{C}=\text{O}$ formation described earlier is attributable to the secondary reaction of HO^* with TME. Note that in the absence of NO , $(\text{CH}_3)_2\text{C}(\text{OH})\text{C}(\text{CH}_3)_2\text{O}^*$ could be formed from the $(\text{CH}_3)_2\text{C}(\text{OH})\text{C}(\text{CH}_3)_2\text{OO}^*$, e.g., $2-(\text{CH}_3)_2\text{C}(\text{OH})\text{C}(\text{CH}_3)_2\text{OO}^* \rightarrow 2(\text{CH}_3)_2\text{C}(\text{OH})\text{C}(\text{CH}_3)_2\text{O}^* + \text{O}_2$. An alternative fate of $(\text{CH}_3)_2\text{C}(\text{OH})\text{C}(\text{CH}_3)_2\text{OO}^*$ in the O_3 -TME-air system is the reaction with the HOO^* , i.e., $(\text{CH}_3)_2\text{C}(\text{OH})\text{C}(\text{CH}_3)_2\text{OO}^* + \text{HOO}^* \rightarrow (\text{CH}_3)_2\text{C}(\text{OH})\text{C}(\text{CH}_3)_2\text{OOH} + \text{O}_2$. In fact, the residual spectrum, Figure 2C, appears to belong largely to this compound. However, this reaction could not be examined in the present photochemical system because of the rapid conversion of $(\text{CH}_3)_2\text{C}(\text{OH})\text{C}(\text{CH}_3)_2\text{OO}^*$ and HOO^* to $(\text{CH}_3)_2\text{C}(\text{OH})\text{C}(\text{CH}_3)_2\text{O}^*$ and HO^* by NO . Clearly, further work is needed to verify this possibility.

Registry No. TME, 563-79-1.

Stopped-Flow Studies of the Mechanisms of Ozone-Alkene Reactions in the Gas Phase: Tetramethylethylene

Richard I. Martinez* and John T. Herron

Chemical Kinetics Division, National Bureau of Standards, Gaithersburg, Maryland 20899

(Received: August 1, 1986)

The reaction of ozone with tetramethylethylene (TME) has been studied in the gas phase at 294 K and 530 Pa (4 Torr) with a stopped-flow reactor coupled to a photoionization mass spectrometer. The concentrations of reactants and products were determined as a function of reaction time. The major products were $(\text{CH}_3)_2\text{CO}$, H_2CO , $\text{CH}_3\text{C}(\text{O})\text{CH}_2\text{OH}$ (hydroxyacetone), and $\text{CH}_3\text{C}(\text{O})\text{C}(\text{O})\text{H}$ (methylglyoxal). Computer simulation of the experimentally observed temporal profiles supports the mechanism shown in Scheme I. The "hot" ester channel $[\text{R}'\text{R}''\text{COO} \rightarrow \text{R}'\text{C}(\text{O})\text{OR}'' \rightarrow \text{products}]$ available to the H_2COO formed by ozonolysis of terminal olefins $\text{R}'\text{R}''\text{C}=\text{CH}_2$ is not available for alkyl-substituted $\text{R}'\text{R}''\text{COO}$. Thus the secondary chemistry for $\text{R}'\text{R}''\text{COO}$ is substantially different from that for H_2COO .

Introduction

The mechanisms of the reactions of ozone with olefins in the gas phase continue to present very serious interpretive problems.¹⁻³

(1) Herron, J. T.; Martinez, R. I.; Huie, R. E. *Int. J. Chem. Kinet.* **1982**, *14*, 201, 225.

(2) Martinez, R. I.; Herron, J. T.; Huie, R. E. *J. Am. Chem. Soc.* **1981**, *103*, 3807.

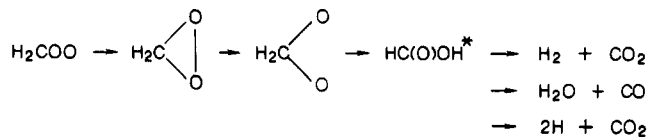
(3) Atkinson, R.; Carter, W. L. *Chem. Rev.* **1986**, *86*, 69.

In earlier work from this laboratory, we developed a detailed mechanism for the ozone-ethylene reaction⁴ that had as its starting point the Criegee mechanism^{5,6} for solution-phase ozonolysis

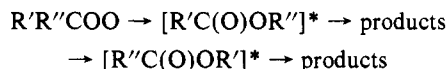


(4) Herron, J. T.; Huie, R. E. *J. Am. Chem. Soc.* **1977**, *99*, 5430.

where POZ is the primary and SOZ the secondary ozonide. It was proposed that in the gas phase at low pressure the reaction leading to SOZ was inoperative and that the fate of the Criegee intermediate was determined by unimolecular loss processes



Extension of this work to propene and isobutene⁷ was not as successful in that the particular Criegee decomposition channels were more difficult to identify unambiguously. We had tentatively proposed a general mechanism involving isomerization of the Criegee intermediate to a "hot" acid or ester than then decomposed.

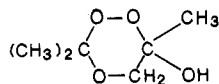


Several comments on these earlier studies are appropriate. First, as we pointed out earlier,^{2,7} it is unlikely that stabilized acids or esters could be primary products of the isomerizations of the Criegee intermediates. The temporal profiles of these species clearly indicate that they arise in secondary processes, probably involving radical ozonolysis or wall interactions. Second, our inability to fit the propene and isobutene data in a truly satisfactory manner indicated that either our knowledge of the secondary chemistry following the isomerization and decomposition of the Criegee intermediate was incomplete or incorrect or other channels may be operative with respect to Criegee isomerization.

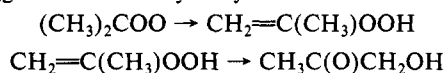
Since that earlier work, we have carried out an extensive mass spectrometric analysis of the products of a broad range of ozone-olefin reactions² which revealed a diversity of products that indicate that, indeed, the mechanism may be more complex. The possible role of an oxygen atom product channel was discussed^{1,2} and was confirmed in an FTIR study of the atmospheric pressure ozonation of *trans*-C₂H₂Cl₂ in which evidence was presented for the reaction $\text{H}(\text{Cl})\text{COO} \rightarrow \text{H}(\text{Cl})\text{C}=\text{O} + \text{O}$.⁸ Oxygen atom production has also been confirmed for $\{\text{Ph}(\text{H})\text{C} + \text{O}_2 \rightarrow \text{Ph}(\text{H})\text{COO} \rightarrow \text{Ph}(\text{H})\text{C}=\text{O} + \text{O}\}$ ⁹ and for $\{\text{H}_2\text{C} + \text{O}_2 \rightarrow \text{H}_2\text{COO} \rightarrow \text{H}_2\text{CO} + \text{O}\}$.^{1,10,11} The possible occurrence of $\{\text{Me}_2\text{COO} \rightarrow \text{Me}_2\text{CO} + \text{O}\}$ has also been discussed.¹

There is also evidence from solution-phase studies that Criegee intermediates can isomerize to products not characteristic of those expected from the formation of hot acids or esters. The best example is tetramethylethylene, which under normal ozonolysis conditions does not yield tetramethylethylene ozonide.

In the reaction of ozone with TME in solution, the secondary ozonide is not formed, but rather the major isolatable products are acetone diperoxide (~15% yield) and higher oligomers of (CH₃)₂COO.⁶ In their study of the reaction, Story and Burgess¹² reported that hydroxyacetone was a minor product (~1% yield) along with a cyclic peroxy alcohol (~10% yield), probably



They suggested that the hydroxyacetone is formed via

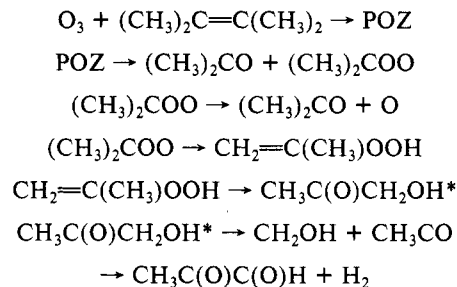


The cyclic peroxy alcohol probably was formed in a secondary reaction involving the Criegee intermediate and hydroxyacetone,⁶ a process unlikely to be of any importance in the gas phase.

A mass spectral peak corresponding to hydroxyacetone (but also to the mass of the Criegee intermediate and to CH₃C(O)-OCH₃) was reported in our earlier mass spectrometric study of the reaction of ozone with tetramethylethylene.²

Here we report a more detailed study of that reaction using stopped-flow mass spectrometry. This work supports the mechanism in Scheme I and indicates that the simple "hot" ester hypothesis needs to be critically reconsidered and probably rejected for alkyl-substituted olefins.

SCHEME I



Experimental Section

The reaction was studied at 294 K and 530 Pa (4 Torr) with a stopped-flow reactor coupled to a photoionization mass spectrometer as described in detail elsewhere.^{2,4} The reactor was a 300 cm³ sphere. Reactants were premixed prior to their entry into the reactor and flowed through the reactor. Gas within the reactor could be isolated by closing simultaneously solenoid valves at the inlet and outlet. The gas within the reactor was sampled continuously through a 200-μm orifice into a photoionization mass spectrometer.

In a typical experiment, a stream of O₂ containing about 1% ozone was flowed through the reactor. A mixture consisting of ca. 4% TME in Ar was then injected into the O₃/O₂ gas flow at a point ca. 90 cm upstream from the sampling orifice of the mass spectrometer. Hence, the reactants are very well mixed long before they enter the reactor. The partial pressure of TME was adjusted so that $[\text{O}_3]_0 \geq 20[\text{TME}]_0$ and pseudo-first-order conditions prevailed. The mass spectrometer was then focused on a particular reactant or product peak in the mass spectrum, the inlet/outlet valves were closed simultaneously, and the temporal profile of each species was obtained in the isolated static reactor. This process was repeated anywhere from 2 to 50 times to build up sufficient signal for each reactant and product. In this way, we developed temporal profiles for the reactants O₃ and TME and the major products (CH₃)₂CO, H₂CO, CH₃C(O)CH₂OH (hydroxyacetone), and CH₃C(O)C(O)H (methylglyoxal). Limiting values were obtained for CO₂. The assignment of mass spectral peaks at *m/e* 74 and 72 to hydroxyacetone and methylglyoxal, respectively, was based on the FTIR atmospheric pressure study of the reaction by Niki et al.,¹³ in which these were found to be major products (yields ~10–20%).

Converting mass spectrometric signals to partial pressure and then concentrations required the use of calibration mixtures. For the stable gases, we used procedures described in ref 4 and 7 and for formaldehyde that described in ref 14.

Experimental Results

The reactor used in this work was a modification of that used in earlier work to enable us to work with reactions faster than O₃ + 2-butene. Figure 1 depicts the decay of TME given as log [TME] vs. the measured experimental time *t*_{exptl}. The zero time here is the time at which the inlet/outlet valves are closed; i.e., *t*_{exptl} = 0. It is evident from Figure 1 that immediately after closure

- (5) Criegee, R. *Angew. Chem., Int. Ed. Engl.* **1975**, *14*, 745.
 (6) Bailey, P. S. *Ozonation in Organic Chemistry*; Academic: New York, 1978; Vol. I; 1982; Vol. II.
 (7) Herron, J. T.; Huie, R. E. *Int. J. Chem. Kinet.* **1978**, *10*, 1019.
 (8) Niki, H.; Maker, P. D.; Savage, C. M.; Breitenbach, L. P.; Martinez, R. I. *J. Phys. Chem.* **1984**, *88*, 766.
 (9) Sander, W. *Angew. Chem., Int. Ed. Engl.* **1985**, *24*, 988.
 (10) Hatakeyama, S.; Bandow, H.; Okuda, M.; Akimoto, H. *J. Phys. Chem.* **1981**, *85*, 2249.
 (11) Martinez, R. I.; Huie, R. E.; Herron, J. T. *J. Chem. Phys.* **1981**, *75*, 5975.
 (12) Story, P. S.; Burgess, J. R. *J. Am. Chem. Soc.* **1967**, *89*, 5726; **1968**, *90*, 1094.

- (13) Niki, H.; Maker, P. D.; Savage, C. M.; Breitenbach, L. P.; Hurley, M. D. *J. Phys. Chem.*, preceding paper in this issue.
 (14) Martinez, R. I.; Herron, J. T. *Int. J. Chem. Kinet.* **1978**, *10*, 433.

TABLE I: Mechanism of the O₃ + TME Reaction: Formation and Loss of the Criegee Intermediate

reaction	model A	model B	model C
1. O ₃ + TME → (CH ₃) ₂ CO + (CH ₃) ₂ COO		1 × 10 ⁹ cm ³ mol ⁻¹ s ⁻¹	
Ester Channel			
2. (CH ₃) ₂ COO → CH ₃ C(O)OCH ₃ *	100%		
3. CH ₃ C(O)OCH ₃ * → CH ₃ CO + CH ₃ O	k ₃ /k ₄ = 4		
4. CH ₃ C(O)OCH ₃ * → CH ₃ C(O)O + CH ₃			
Oxygen-Atom Channel			
5. (CH ₃) ₂ COO → (CH ₃) ₂ CO + O			20%
Hydroperoxide Channel			
6. (CH ₃) ₂ COO → CH ₂ =C(CH ₃)OOH		100%	80%
7. CH ₂ =C(CH ₃)OOH → CH ₂ =C(CH ₃)O + OH		k ₇ /k ₈ = 0.43	
8. CH ₂ =C(CH ₃)OOH → CH ₃ C(O)CH ₂ OH*		fast	fast
9. CH ₃ C(O)CH ₂ OH* → CH ₃ OH + CH ₃ CO		fast	
10. CH ₃ C(O)CH ₂ OH* → CH ₃ C(O)C(O)H + H ₂			k ₉ /k ₁₀ /k ₁₁ = 11/1.3/1
11. CH ₃ C(O)CH ₂ OH* \xrightarrow{M} CH ₃ C(O)CH ₂ OH			
Δ[CO ₂]/Δ[TME] at t = 5.4 s	0.80	0.51	0.46

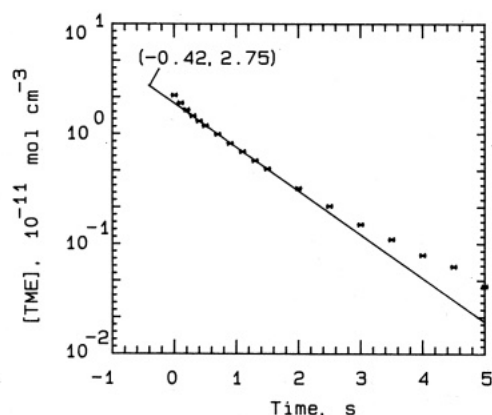


Figure 1. log [TME] vs. t_{expt} . Reaction time $t = 0$ corresponds to $t_{\text{expt}} = -0.42$ s.

(0 s < t_{expt} < 0.2 s) the isolated static reactor lacked homogeneity, even though the flowing reactants were very well mixed long before they entered the reactor. This is as it should be. For any flowing reactor, no matter how well mixed the reactants are, there will always be reactant concentration gradients between the inlet and outlet valves due to the relatively fast reactions taking place as the reacting gas mixture flows downstream. These concentration gradients disappeared through diffusional mixing within 0.2 s after the reactor was isolated, as evidenced by the fact that the isolated reactor is kinetically well behaved after the first 0.2 s following closure of the inlet/outlet valves (i.e., pseudo-first-order conditions prevailed for 0.2 s < t_{expt} < 2 s).

In order to model the data, we must start our modeling calculations at true reaction time zero (i.e., from the point of admixture of the very dilute O₃/O₂ and TME/Ar mixtures). Moreover, the model assumes well-mixed reactants from true reaction time zero. At 4 Torr total pressure, the diffusivity is sufficiently large that the reactants should in fact be very well mixed long before they enter the flowing reactor and certainly within milliseconds downstream from the point of admixture of the very dilute mixtures of O₃/O₂ [ca. 0.3% mol of O₃ at 4 Torr] and TME/Ar [ca. 0.01% mol of TME at 4 Torr]. These are sufficiently dilute that there cannot be any significant thermal gradients at the point of their admixture and certainly none within the reactor. Therefore, it is highly unlikely that regions of elevated temperatures and/or high free radical concentrations can ever be formed in our reactor under these conditions. Hence, despite the short-lived (0 s < t_{expt} < 0.2 s) local inhomogeneity that is observed upon closure of the inlet/outlet valves and that is due to the transition from *flowing* reactor (with concentration gradients) to homogeneous, isolated *static* reactor (with no gradients), it is evident that well-behaved pseudo-first-order conditions prevailed throughout and certainly for $t_{\text{expt}} < 0$ s and $t_{\text{expt}} > 0.2$ s. Consequently, there is every reason to believe (a) that the observed

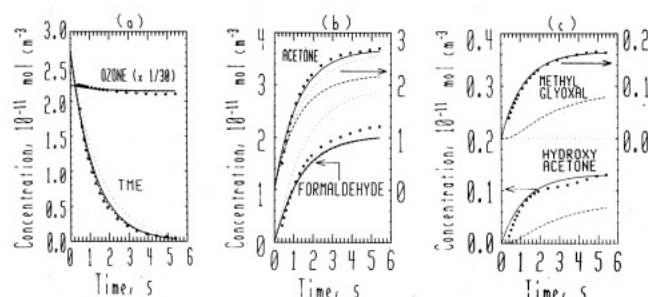


Figure 2. Temporal profiles of the concentrations of reactants and products for the reaction of O₃ with tetramethylethylene (TME) at 294 K and 4 Torr; [O₃]₀ = 2.2 × 10⁻⁷ mol cm⁻³: (**) experimental data; (---) model A (see Modeling and Table I); (---) model B (see Modeling and Table I); (—) model C (see Modeling and Table I).

temporal profiles of reactant and product concentrations are correct and true (i.e., not somehow masked by flow/no-flow aberrations) for $t_{\text{expt}} < 0$ s and $t_{\text{expt}} > 0.2$ s and (b) that the pseudo-first-order line of Figure 1 (0.2 s < t_{expt} < 2 s) can be back-extrapolated to intersect the true reaction time zero at the known [TME]₀. Therefore, for [TME]₀ = 2.75 × 10⁻¹¹ mol cm⁻³, the true reaction time zero, $t = 0$, corresponds to $t_{\text{expt}} \approx -0.4$ s as indicated by the solid line in Figure 1. That is, it takes ca. 0.4 s for the reacting mixture of O₃ + TME to flow from the point of admixture of the dilute O₃/O₂ and TME/Ar mixtures to the sampling orifice of the mass spectrometer. This is consistent with the flow times previously estimated. In what follows, we have redefined the absolute reaction time zero of our experiments in this manner.

It should be noted that the effective specific rate constant for TME + O₃ that can be derived from the solid rectilinear part of the plot is $k = 1.4 \times 10^9$ cm³ mol⁻¹ s⁻¹. This is considerably higher than literature values [(6–9) × 10⁸ cm³ mol⁻¹ s⁻¹,^{15,16}] and indicates that TME is being removed in secondary free radical reactions. In the modeling studies that are discussed next, we used a value of 10⁹ cm³ mol⁻¹ s⁻¹, which is about 10% higher than the highest experimental value.¹⁷

In Figure 2 we show the temporal profiles for the reactants and major products; here $t = 0$ is the absolute reaction time zero (corresponds to $t_{\text{expt}} \approx -0.4$ s). The experimental data are in-

(15) Japar, S. M.; Wu, C. H.; Niki, H. *J. Phys. Chem.* **1974**, *78*, 2318.

(16) Huie, R. E.; Herron, J. T. *Int. J. Chem. Kinet.* (Symp. No. 1) **1975**, *165*.

(17) The reported rate constants for O₃ + olefin reactions^{15–19} differ significantly, particularly for the internal olefins such as TME. There appear to be systematic sources of error that are not understood, and rate constants for the faster reactions are therefore unreliable. Additional measurements are clearly needed.

(18) Adenji, S. A.; Kerr, J. A.; Williams, M. R. *Int. J. Chem. Kinet.* **1981**, *13*, 209.

(19) Atkinson, R.; Aschmann, S. M.; Carter, W. P. L.; Pitts, J. N., Jr. *Int. J. Chem. Kinet.* **1983**, *15*, 721.

indicated by asterisks. The other curves are the results of modeling calculations to be described next. The upper limit for the yield of CO_2 was estimated to be <0.9 mol per mole of TME consumed; this yield of CO_2 can be accommodated by any of the models (See Table I). No other products were found in significant yield.

Modeling

In order to arrive at a mechanism to explain the observed temporal profiles, we have carried out a series of modeling studies using the HICHM program of Brown.²⁰

We start with the assumption that the initial step involves the formation of 1,2,3-trioxolane (POZ), which under our conditions decomposes to acetone and the Criegee diradical



The subsequent chemistry of the $(\text{CH}_3)_2\text{COO}$ intermediate gives rise to all the other products observed.

To clarify the modeling results, we have separated the chemical kinetic model into two parts. The first part, representing unimolecular isomerization and/or decomposition channels available to the Criegee intermediate, is given in Table I. The second and much more extensive part, which includes all the secondary radical-molecule or radical-radical reactions, is given in Table II. The sources of these data are also given. For the modeling calculations, the branching ratios for the channels given in Table I are the only parameters that are varied. All of the kinetic parameters for the reactions in Table II were held constant.

In modeling the reactions, we first considered the mechanism involving formation of a "hot" ester followed by decomposition, i.e., reaction 1-4 in Table I. The only variable is the ratio k_3/k_4 . The best fit was obtained by using the ratio given in model A of Table I. The model A results shown in Figure 2 for the ester channel seem to rule out that channel conclusively. The decay of TME is much too slow, the yield of H_2CO much too large, and the model fails completely to predict the formation of methylglyoxal or hydroxyacetone.

The observed rapid decay of TME in comparison to the much slower decay predicted by model A strongly indicates that secondary reactions are responsible for the excess loss of TME. However, the only possible reaction products that could react rapidly with TME under our experimental conditions are O and OH. If all of the Criegee intermediate were lost via reaction 5, then again there would be no significant source terms in the secondary reactions of Table II for the minor products or for H_2CO . Thus, addition of reaction 5, which would enhance the TME decay rate, does nothing to explain the observed temporal profiles of the products.

At the next level of complexity, we can introduce reactions based on the solution-phase studies which invoke the tautomerization of the Criegee intermediate to the methyl-substituted vinyl hydroperoxide, reaction 6. The vinyl hydroperoxide can react in several ways. It can decompose as in reaction 7 to provide a source of reactive OH radicals and (methylvinyl)oxy radicals. The latter can in turn react to produce methylglyoxal and hydroxyacetone in secondary reactions (See Table II). Extensive modeling calculations for the hydroperoxide channel were made by using reactions 6 and 7 and combinations of it with reactions 2-5. The best fit obtained is shown in Table I and Figure 2 as model B. The fit to the TME decay rate is acceptable and to H_2CO is excellent but is much too low with regard to acetone and the two lesser products, hydroxyacetone and methylglyoxal. For the latter two products, examination of the shapes of the predicted curves indicates that they have the sigmoidal shape we would expect for secondary products formed in a complex radical-radical reaction sequence. The experimental data do not seem to share this characteristic. They suggest that these are "prompt" products resulting from sequential isomerizations subsequent to Me_2COO production. Reactions 8-11 therefore were included and reaction

7 dropped. The best fit using this mechanism, again including reactions 2-5 in various ratios, is given as model C in Table I and is shown in Figure 2. In this case, the fits to all species are very close.

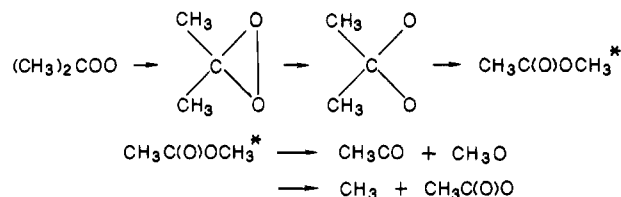
The observation of O-atom production from $\text{H}(\text{Cl})\text{COO}$,⁸ $\text{Ph}(\text{H})\text{COO}$,⁹ and H_2COO ,^{10,11} lends further credence to the probable involvement of $\text{Me}_2\text{COO} \rightarrow \text{O} + \text{Me}_2\text{CO}$ as used in model C in Table I.

Discussion

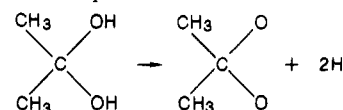
In itself, modeling cannot define unambiguously the chemistry of any system as complex as the O_3 -TME reaction. It can help however in defining which reactions are possible and which are clearly not.

We consider the reactions in Table I in terms of their thermochemistry and chemical kinetics. Derived thermochemical data are given in Table III and discussed below. Data on other species used in the calculations were taken from ref 21-23.

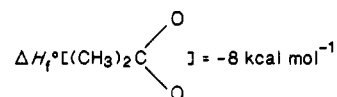
In considering the Criegee isomerization mechanism leading to "hot" acids or esters, i.e.



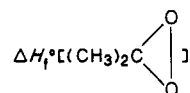
we start with the assumption that for the reaction



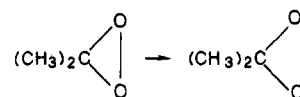
the reaction enthalpy change can be equated to twice the $\text{CH}_3\text{O}-\text{H}$ bond strength in methanol²¹ ($2 \times 104 = 208 \text{ kcal mol}^{-1}$). On this basis we obtain



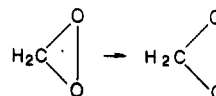
We obtained



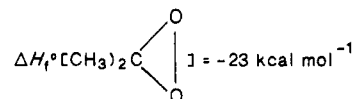
by assuming that the heat of the reaction



was the same as we had earlier deduced¹ for the comparable dioxirane reaction



i.e., 15 kcal mol^{-1} . It follows that



For planar $(\text{CH}_3)_2\text{COO}$, the initially formed Criegee intermediate, we accept the value of $\Delta H_f^\circ = 3.6 \text{ kcal mol}^{-1}$, estimated by Nangia and Benson.²⁷

(20) Brown, R. L. *HICHM: A Fortran Code for Homogeneous Isothermal Chemical Kinetics Systems*; National Bureau of Standards: Gaithersburg, MD 20899, 1981; NBSIR 81-2281.

(21) McMillen, D. F.; Golden, D. M. *Annu. Rev. Phys. Chem.* **1982**, *33*, 493.

(22) Benson, S. W. *Thermochemical Kinetics*; Wiley: New York, 1976.

(23) Cox, J. D.; Pilcher, G. *Thermochemistry of Organic and Organometallic Compounds*; Academic: New York, 1970.

TABLE II: Mechanism of the O₃-TME Reaction: Secondary Processes

reaction	rate const ^a	ref
12. H ₂ C=C(Me)O = MeC(O)CH ₂	1.0 × 10 ¹⁴	<i>b</i>
13. MeC(O)CH ₂ + O ₂ = MeC(O)CH ₂ OO	4.2 × 10 ¹²	<i>c</i> [<i>d-g</i>]
14. 2MeC(O)CH ₂ OO = 2MeC(O)CH ₂ O + O ₂	3.0 × 10 ¹⁰	<i>c</i> [<i>h</i>]
15. 2MeC(O)CH ₂ OO = MeC(O)CH ₂ OH + MeC(O)C(O)H + O ₂	3.0 × 10 ¹⁰	<i>c</i> [<i>h</i>]
16. MeC(O)CH ₂ O + O ₂ = HO ₂ + MeC(O)C(O)H	4.8 × 10 ⁹	<i>c</i> [<i>h, i</i>]
17. OH + MeC(O)C(O)H = H ₂ O + MeC(O)C(O)	9.0 × 10 ¹²	<i>f</i>
18. OH + MeC(O)CH ₂ OH = H ₂ O + MeC(O)CH(OH)	2.9 × 10 ¹¹	<i>c</i> [<i>g, h</i>]
19. MeC(O)CH(OH) + O ₂ = MeC(O)CH(OH)OO	7.0 × 10 ¹²	<i>c</i> [<i>d-f</i>]
20. MeC(O)CH(OH)OH = H ₂ O + MeC(O)C(O)H	1.0 × 10 ¹⁴	<i>b</i>
21. MeC(O)CH(OH)O + O ₂ = HO ₂ + MeC(O)C(O)OH	4.8 × 10 ⁹	<i>c</i> [<i>h, i</i>]
22. MeC(O)CH(OH)O = MeC(O) + HCOOH	1.0 × 10 ³	<i>c</i> [<i>h</i>]
23. MeC(O)CH ₂ O = MeC(O) + H ₂ CO	1.0 × 10 ⁴	<i>c</i> [<i>h</i>]
24. MeC(O)CH ₂ O = CH ₂ C(O)CH ₂ OH	1.0 × 10 ²	<i>c</i> [<i>h</i>]
25. MeC(O) + O ₂ = MeC(O)OO	1.2 × 10 ¹²	<i>j</i>
26. 2MeC(O)OO = 2MeC(O)O + O ₂	1.2 × 10 ¹²	<i>h</i>
27. MeC(O)O = Me + CO ₂	1.0 × 10 ⁹	<i>b</i>
28. Me + O ₂ = MeO ₂	2.7 × 10 ¹⁰	<i>k</i>
29. 2MeO ₂ = 2MeO + O ₂	9.0 × 10 ¹⁰	<i>g</i>
30. 2MeO ₂ = MeOH + H ₂ CO + O ₂	1.3 × 10 ¹¹	<i>g</i>
31. 2MeO ₂ = MeOOME + O ₂	1.8 × 10 ¹⁰	<i>g</i>
32. MeC(O)OO + MeO ₂ = MeC(O)O + MeO + O ₂	6.0 × 10 ¹⁰	<i>h</i>
33. MeO + O ₂ = H ₂ CO + HO ₂	9.0 × 10 ⁸	<i>g, i</i>
34. OH + H ₂ CO = H ₂ O + HCO	6.6 × 10 ¹²	<i>g</i>
35. HCO + O ₂ = HO ₂ + CO	3.1 × 10 ¹²	<i>g</i>
36. CO + OH = CO ₂ + H	9.0 × 10 ¹⁰	<i>g</i>
37. H + O ₂ = HO ₂	4.7 × 10 ⁹	<i>g</i>
38. HO ₂ + O ₃ = OH + O ₂	1.2 × 10 ⁹	<i>g</i>
39. OH + O ₃ = HO ₂ + O ₂	4.0 × 10 ¹⁰	<i>g</i>
40. HO ₂ + OH = H ₂ O + O ₂	4.8 × 10 ¹³	<i>g</i>
41. H + O ₃ = OH + O ₂	1.7 × 10 ¹³	<i>g</i>
42. MeC(O)C(O) + O ₂ = MeC(O)C(O)OO	1.0 × 10 ¹²	<i>c</i> [<i>d-f, j</i>]
43. 2MeC(O)C(O)OO = 2MeC(O)C(O)O + O ₂	1.3 × 10 ¹³	<i>c</i> [<i>h</i>]
44. MeC(O)C(O)O = MeC(O) + CO ₂	1.0 × 10 ⁹	<i>b</i>
45. OH + Me ₂ CO = H ₂ O + MeC(O)CH ₂	1.7 × 10 ¹¹	<i>h</i>
46. OH + TME = Me ₂ C(OH)C(Me) ₂	7.2 × 10 ¹³	<i>l</i>
47. Me ₂ C(OH)C(Me) ₂ + O ₂ = Me ₂ C(OH)C(Me) ₂ OO	1.8 × 10 ¹³	<i>c</i> [<i>d</i>]
48. Me ₂ C(OH)C(Me) ₂ O = Me ₂ CO + Me ₂ C(OH)	1.0 × 10 ⁴	<i>c</i> [<i>h</i>]
49. Me ₂ C(OH) + O ₂ = Me ₂ CO + HO ₂	1.2 × 10 ¹³	<i>c</i> [<i>d</i>]
50. OH + MeC(O)CH ₂ OH = H ₂ O + CH ₂ C(O)CH ₂ OH	1.7 × 10 ¹¹	<i>c</i> [<i>g, h, l</i>]
51. MeO ₂ + MeO = MeOOH + H ₂ CO	7.9 × 10 ¹²	<i>m</i>
52. OH + MeOOH = MeO ₂ + H ₂ O	4.2 × 10 ¹¹	<i>n</i>
53. OH + MeOOH = CH ₂ OOH + H ₂ O	4.2 × 10 ¹¹	<i>n</i>
54. CH ₂ OOH = H ₂ CO + OH	1.0 × 10 ⁹	<i>o</i>
55. MeO ₂ + HO ₂ = MeOOH + O ₂	3.9 × 10 ¹²	<i>g</i>
56. MeO + HO ₂ = H ₂ CO + H ₂ O ₂	1.0 × 10 ¹³	<i>c</i> [<i>m</i>]
57. OH + H ₂ O ₂ = H ₂ O + HO ₂	1.0 × 10 ¹²	<i>g</i>
58. OH + MeOH = CH ₂ OH + H ₂ O	6.0 × 10 ¹¹	<i>g</i>
59. OH + MeOH = MeO + H ₂ O	6.0 × 10 ¹⁰	<i>c</i> [<i>g</i>]
60. CH ₂ OH + O ₂ = HO ₂ + H ₂ CO	1.2 × 10 ¹²	<i>g</i>
61. HO ₂ + MeC(O)CH ₂ OO = O ₂ + MeC(O)CH ₂ OOH	6.0 × 10 ¹¹	<i>c</i> [<i>g</i>]
62. MeC(O)CH ₂ OOH + OH = MeC(O)CH ₂ OO + H ₂ O	4.2 × 10 ¹¹	<i>c</i> [<i>n</i>]
63. MeC(O)CH ₂ OOH + OH = MeC(O)C(H)(OOH) + H ₂ O	4.2 × 10 ¹¹	<i>c</i> [<i>n</i>]
64. MeC(O)C(H)(OOH) = MeC(O)C(O)H + OH	1.0 × 10 ⁹	<i>c</i> [<i>o</i>]
65. HO ₂ + MeC(O)CH ₂ O = MeC(O)C(O)H + H ₂ O ₂	1.0 × 10 ¹³	<i>c</i> [<i>m</i>]
66. HO ₂ + MeC(O)OO = MeC(O)OOH + O ₂	6.0 × 10 ¹¹	<i>c</i> [<i>g</i>]
67. MeC(O)OOH + OH = MeC(O)OO + H ₂ O	4.2 × 10 ¹¹	<i>c</i> [<i>n</i>]
68. MeC(O)C(O)OO + HO ₂ = MeC(O)C(O)OOH + O ₂	6.0 × 10 ¹¹	<i>c</i> [<i>g</i>]
69. OH + MeC(O)C(O)OOH = H ₂ O + MeC(O)C(O)OO	4.2 × 10 ¹¹	<i>c</i> [<i>n</i>]
70. HO ₂ + Me ₂ C(OH)C(Me) ₂ OO = O ₂ + Me ₂ C(OH)C(Me) ₂ OOH	6.0 × 10 ¹¹	<i>c</i> [<i>g</i>]
71. Me ₂ C(OH)C(Me) ₂ OOH + OH = H ₂ O + Me ₂ C(OH)C(Me) ₂ OO	4.2 × 10 ¹¹	<i>c</i> [<i>n</i>]
72. MeO ₂ + MeC(O)CH ₂ OO = MeO + MeC(O)CH ₂ O + O ₂	2.4 × 10 ¹⁰	<i>c</i> [<i>h</i>]
73. MeO ₂ + MeC(O)CH ₂ OO = MeOH + MeC(O)C(O)H + O ₂	1.8 × 10 ¹⁰	<i>c</i> [<i>h</i>]
74. MeO ₂ + MeC(O)CH ₂ OO = H ₂ CO + MeC(O)CH ₂ OH + O ₂	1.8 × 10 ¹⁰	<i>c</i> [<i>h</i>]
75. MeO ₂ + MeC(O)CH ₂ O = MeOOH + MeC(O)C(O)H	1.0 × 10 ¹³	<i>c</i> [<i>m</i>]
76. MeO ₂ + MeC(O)OO = MeO + MeC(O)O + O ₂	3.0 × 10 ¹⁰	<i>c</i> [<i>h</i>]
77. MeO ₂ + MeC(O)OO = H ₂ CO + MeC(O)OH + O ₂	3.0 × 10 ¹⁰	<i>c</i> [<i>h</i>]
78. MeO ₂ + MeC(O)C(O)OO = MeO + MeC(O)C(O)O + O ₂	3.0 × 10 ¹⁰	<i>c</i> [<i>h</i>]
79. MeO ₂ + Me ₂ C(OH)C(Me) ₂ OO = MeO + Me ₂ C(OH)C(Me) ₂ O + O ₂	3.0 × 10 ¹⁰	<i>c</i> [<i>h</i>]
80. MeO ₂ + Me ₂ C(OH)C(Me) ₂ OO = H ₂ CO + Me ₂ C(OH)C(Me) ₂ OH + O ₂	3.0 × 10 ¹⁰	<i>c</i> [<i>h</i>]
81. 2HO ₂ = H ₂ O ₂ + O ₂	1.5 × 10 ¹²	<i>g</i>
82. MeO + MeC(O)CH ₂ OO = H ₂ CO + MeC(O)CH ₂ OOH	1.0 × 10 ¹³	<i>c</i> [<i>m</i>]
83. MeO + MeC(O)OO = H ₂ CO + MeC(O)OOH	1.0 × 10 ¹³	<i>c</i> [<i>m</i>]
84. MeO + MeC(O)C(O)OO = H ₂ CO + MeC(O)C(O)OOH	1.0 × 10 ¹³	<i>c</i> [<i>m</i>]
85. MeO + Me ₂ C(OH)C(Me) ₂ OO = H ₂ CO + Me ₂ C(OH)C(Me) ₂ OOH	1.0 × 10 ¹³	<i>c</i> [<i>m</i>]
86. Me + O ₃ = MeO + O ₂	1.8 × 10 ¹²	<i>p</i>
87. MeC(O)CH ₂ + O ₃ = MeC(O)CH ₂ O + O ₂	1.8 × 10 ¹³	<i>c</i> [<i>p</i>]

TABLE II (Continued)

reaction	rate const ^a	ref
88. MeC(O)CH(OH) + O ₃ = MeC(O)CH(OH)O + O ₂	1.8 × 10 ¹³	c [p]
89. MeC(O) + O ₃ = MeC(O)O + O ₂	1.8 × 10 ¹³	c [p]
90. HCO + O ₃ = HCOO + O ₂	1.8 × 10 ¹³	c [p]
91. HCOO = H + CO ₂	1.0 × 10 ⁹	b
92. MeC(O)C(O) + O ₃ = MeC(O)C(O)O + O ₂	1.8 × 10 ¹³	c [p]
93. Me ₂ C(OH)C(Me) ₂ + O ₃ = Me ₂ C(OH)C(Me) ₂ O + O ₂	3.0 × 10 ¹³	c [p]
94. Me ₂ C(OH) + O ₃ = Me ₂ C(OH)O + O ₂	1.8 × 10 ¹³	c [p]
95. Me ₂ C(OH)O = Me + MeC(O)OH	1.0 × 10 ⁵	b
96. CH ₂ OH + O ₃ = OCH ₂ OH + O ₂	1.8 × 10 ¹²	c [p]
97. OCH ₂ OH + O ₂ = HO ₂ + HCOOH	3.6 × 10 ⁸	c [g-i]
98. MeO ₂ + MeC(O)CH(OH)OO = MeO + MeC(O)CH(OH)O + O ₂	3.0 × 10 ¹⁰	c [h]
99. MeO ₂ + MeC(O)CH(OH)OO = H ₂ CO + MeC(O)CH(OH)OH + O ₂	3.0 × 10 ¹⁰	c [h]
100. O + TME = MeC(O)C(Me) ₂ + Me	4.8 × 10 ¹³	q-s
101. O + H ₂ CO = OH + HCO	9.6 × 10 ¹⁰	h
102. O + Me ₂ CO = OH + MeC(O)CH ₂	4.0 × 10 ⁸	t
103. O + O ₃ = 2O ₂	5.0 × 10 ⁹	g
104. MeC(O)C(Me) ₂ OO + HO ₂ = O ₂ + MeC(O)C(Me) ₂ OOH	6.0 × 10 ¹¹	c [g]
105. OH + MeC(O)C(Me) ₂ OOH = H ₂ O + MeC(O)C(Me) ₂ OO	4.2 × 10 ¹¹	c [n]
106. MeC(O)C(Me) ₂ OO + MeO ₂ = MeO + MeC(O)C(Me) ₂ O + O ₂	3.0 × 10 ¹⁰	c [h]
107. MeC(O)C(Me) ₂ OO + MeO ₂ = H ₂ CO + MeC(O)C(Me) ₂ OH + O ₂	3.0 × 10 ¹⁰	c [h]
108. MeC(O)C(Me) ₂ O = MeC(O) + Me ₂ CO	1.0 × 10 ⁹	b
109. MeC(O)C(Me) ₂ + O ₂ = MeC(O)C(Me) ₂ OO	1.8 × 10 ¹³	c [d-f]
110. MeC(O)C(Me) ₂ + O ₃ = MeC(O)C(Me) ₂ O + O ₂	3.2 × 10 ¹³	c [p]
111. Me ₂ C(OH)O = Me ₂ CO + OH	1.0 × 10 ⁵	b
112. OH + MeC(O)C(Me) ₂ OH = H ₂ O + MeC(O)C(Me) ₂ O	6.0 × 10 ¹²	c [h, l]
113. O + Me ₂ C(OH)C(Me) ₂ OH = H ₂ O + Me ₂ C(OH)C(Me) ₂ O	6.0 × 10 ¹²	c [h, l]
114. MeO = CH ₂ OH	8.0	i

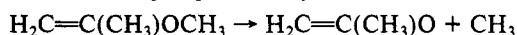
^as⁻¹ (unimolecular); cm³ mol⁻¹ s⁻¹ (bimolecular). ^bEstimated (this work). ^cEstimated (this work) based on data on related compounds in references cited in brackets. ^dLenhardt, T. M.; McDade, C. E.; Bayes, K. D. *J. Chem. Phys.* **1980**, *72*, 304. ^eRuiz, R. P.; Bayes, K. D. *J. Phys. Chem.* **1984**, *88*, 2592. ^fPlumb, I. C.; Ryan, K. R. *Int. J. Chem. Kinet.* **1981**, *13*, 1011; **1982**, *14*, 861. ^gBaulch, D. L.; Cox, R. A.; Crutzen, P. J.; Hampson, R. F., Jr.; Kerr, J. A.; Troe, J.; Watson, R. T. *J. Phys. Chem. Ref. Data* **1982**, *11*, 327; **1984**, *13*, 1259. ^hAtkinson, R.; Lloyd, A. C. *J. Phys. Chem. Ref. Data* **1984**, *13*, 315. ⁱGutman, D.; Sanders, N.; Butler, J. E. *J. Phys. Chem.* **1982**, *86*, 66. ^jMcDade, C. E.; Lenhardt, T. M.; Bayes, K. D. *J. Photochem.* **1982**, *20*, 1. ^kSelzer, E. A.; Bayes, K. D. *J. Phys. Chem.* **1983**, *87*, 392. ^lAtkinson, R.; Darnall, K. R.; Lloyd, A. C.; Winer, A. M.; Pitts, J. N., Jr. *Adv. Photochem.* **1979**, *11*, 375. ^mKerr, J. A.; Moss, S. J., Eds *CRC Handbook of Bimolecular and Termolecular Gas Reactions*; CRC Press: Boca Raton, FL, 1981; Vol. II. ⁿDeMore, W. B.; Watson, R. T.; Golden, D. M.; Hampson, R. F.; Kurylo, M.; Howard, C. J.; Molina, M. J.; Ravishankara, A. R. JPL Publication 82-57, 1982. ^oNiki, H., private communication. ^pPaltenghi, R.; Ogryzlo, E. A.; Bayes, K. D. *J. Phys. Chem.* **1984**, *88*, 2595. ^qHerron, J. T.; Huie, R. E. *J. Phys. Chem. Ref. Data* **1973**, *2*, 467. ^rCvetanovic, R. J. *Rev. Chem. Intermed.* **1984**, *5*, 183; *Can. J. Chem.* **1958**, *36*, 623. ^sCvetanovic, R. J., private communication. ^tLee, J. H.; Timmons, R. B. *Int. J. Chem. Kinet.* **1977**, *9*, 133.

TABLE III: Thermochemical Data^a

species	ΔH_f° , kcal mol ⁻¹	source
(CH ₃) ₂ COO	3.6	ref 27
(CH ₃) ₂ C	-23	bond strengths ¹
(CH ₃) ₂ C	-8	bond strengths
CH ₂ =C(CH ₃)OOH	-25	bond strengths
CH ₂ =C(CH ₃)O	12	bond strengths
CH ₃ C(O)CH ₂ OH	-88	bond strengths
H ₂ C=C(CH ₃)OCH ₃	-34.9	bond strengths
(CH ₃) ₂ C(OH) ₂	-112	group additivity
(CH ₃) ₃ COO	-20.5	ref 28

^aAll values estimated except as shown.

For the species involved in the reaction sequence 6-11, the starting point was the ether, H₂C=C(CH₃)OCH₃, for which ΔH_f° was estimated with group additivity.²⁴ Then for the reaction



equating the heat of reaction to $D(\text{RO}-\text{CH}_3) = 82 \text{ kcal mol}^{-1}$ ²¹ leads to $\Delta H_f^\circ[\text{H}_2\text{C}=\text{C}(\text{CH}_3)\text{O}]$ of 12 kcal mol⁻¹.

To obtain the heat of formation of the hydroperoxide, we consider the reaction

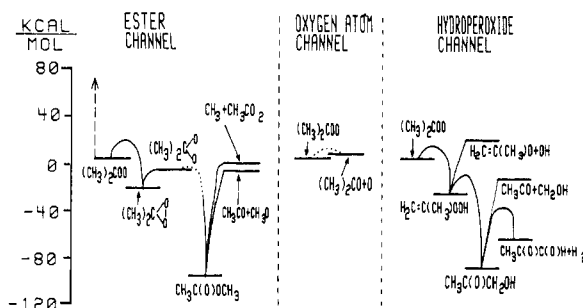
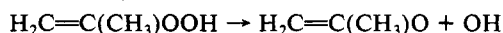


Figure 3. Energy diagrams for possible reaction channels accessible to the Criegee intermediate initially formed in the O₃ + TME reaction (see Discussion).

and, equating the heat of reaction with $D(\text{RO}-\text{OH}) = 46 \text{ kcal mol}^{-1}$,²¹ obtain $\Delta H_f^\circ = -25 \text{ kcal mol}^{-1}$.

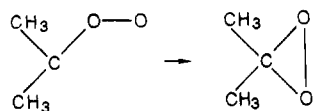
The heat of formation of hydroxyacetone was estimated by assuming that $\Delta H_f^\circ[(\text{CH}_3)_2\text{CO}] - \Delta H_f^\circ[\text{CH}_3\text{C}(\text{O})\text{CH}_2\text{OH}] = \Delta H_f^\circ[\text{C}_2\text{H}_6] - \Delta H_f^\circ[\text{C}_2\text{H}_5\text{OH}]$, from which we obtain $\Delta H_f^\circ[\text{CH}_3\text{C}(\text{O})\text{CH}_2\text{OH}] = -88 \text{ kcal mol}^{-1}$.

These data allow us to construct the energy diagrams shown in Figure 3 for the different possible reaction channels: isomerization to and decomposition of a "hot" ester; bond scission to acetone and an oxygen atom; isomerization to the hydroperoxide followed by competing unimolecular dissociation reactions.

The availability of a particular channel will depend on the amount of internal energy in the initially formed Criegee intermediate and the critical energy required for the reaction to go at a competitive rate. We will consider the case of the Criegee intermediates formed with 34 kcal mol⁻¹ of excess energy (¹/₂ of the exothermicity of reaction, 68 kcal mol⁻¹).

(24) Benson, S. W.; Cruickshank, F. R.; Golden, D. M.; Haugen, G. R.; O'Neal, H. E.; Rodgers, A. S.; Shaw, R.; Walsh, R. *Chem. Rev.* **1969**, *69*, 279.

For the "hot" ester channel, the activation energy for conversion of the initially formed Criegee intermediate to dioxirane



has been taken to be 16 kcal mol⁻¹ based on our previous work¹ on the ethylene ozonolysis reaction. If the Criegee intermediate is formed initially "hot", then it can easily overcome this barrier and isomerize to the "hot" ester which will decompose. The stabilized Criegee, on the other hand, may be relatively stable at room temperature in terms of isomerization to dimethyldioxirane. The computer simulations suggest that the hot ester is not formed, but rather that the competing unimolecular reactions leading to either oxygen atoms and/or hydroperoxide predominate (see Figure 3).

If we accept the implications of the computer simulation, we can obtain zeroth-order estimates for the size of the barriers involved in the various channels.

For example, for isomerization of the Criegee intermediate to the hydroperoxide, we estimate the A factor to be about 10¹² s⁻¹. If we take $k(\text{hydroperoxide}) = 10k(\text{dioxirane})$, consistent with the apparent absence of the ester channel, then the barrier to forming the hydroperoxide is calculated to be ~ 13 kcal mol⁻¹, since the A factor for isomerization of the Criegee intermediate to dioxirane has been estimated to be $\sim 10^{13}$ s⁻¹ and its activation energy to be about 16 kcal mol⁻¹.¹

If we examine Figure 3, we see that the initially formed hydroperoxide can be quenched, can dissociate to produce OH radicals, or can further isomerize to hydroxyacetone. We can treat these reactions in terms of RRK theory following the approach used by Benson.²² We write

$$k = A \left\{ \frac{E - E^*}{E} \right\}^{s-1}$$

where E is the total energy of the reaction complex, E^* the activation energy, and s the number of effective internal degrees of freedom. For "hot" molecules, the value of s is difficult to estimate. Benson²² suggests using $s_{\text{eff}} = (C_p - 8)/R$. There are no data for the hydroperoxide and no group values available to make an estimate. However, at high temperatures $C_p[\text{CH}_2=\text{C}(\text{CH}_3)\text{OOH}] \approx C_p[\text{CH}_3\text{C}(\text{O})\text{CH}_2\text{OH}]$ and the latter can be estimated by comparison of the known C_p s for acetone and ethanol. We can estimate the effective vibrational temperature from the expression

$$\int_0^T (C_p - 8) dt = E^{**}$$

where E^{**} is the thermal energy of the vibrationally excited molecule (none of the energy goes into rotational or vibrational degrees of freedom).

If we consider the case where the initially formed Criegee intermediate [planar (CH₃)₂COO] has 34 kcal of excess energy, then for the hydroperoxide $E = 63$ kcal mol⁻¹. For the bond-breaking reaction leading to OH formation, we estimate $E^* = 46$ kcal mol⁻¹ (i.e., the heat of reaction). Then $E^{**} = 17$ kcal mol⁻¹ and the temperature for which

$$\int_0^T (C_p - 8) dt = 17000 \text{ cal mol}^{-1}$$

is about 850 K. At this temperature $C_p \approx 40$ cal mol⁻¹ K⁻¹, and $s_{\text{eff}} = (C_p - 8)/R = 16$. If we take the A factor to be 10^{15.5} s⁻¹ by analogy with alkyl hydroperoxide decomposition reactions,²⁵ then

$$k = 10^{15.5} \left\{ \frac{63 - 46}{63} \right\}^{15} = 10^{6.97} \text{ s}^{-1}$$

The collision rate at 4 Torr and 300 K is about 10^{7.7} s⁻¹, about 5 times faster, so that the hydroperoxide decomposition channel would have difficulty competing with quenching of the hydroperoxide. As the degree of quenching of the initially formed Criegee intermediate increases (higher pressure), the less favorable becomes the hydroperoxide decomposition channel. At atmospheric pressure, where $Z \sim 10^{10}$ s⁻¹, all of the hydroperoxide will be stabilized unless there are competing unimolecular channels.

There is really no way of estimating a priori what the rate parameters are for the alternate unimolecular channel involving the isomerization of the hydroperoxide to the hydroxyacetone. Since the hydroperoxide was not found in solution ozonolysis studies whereas hydroxyacetone was found as a product, we can only assume that the reaction is fast even for the thermalized system. If we set a half-life for the hydroxyperoxide of 1 h and take the A factor to be 10¹² s⁻¹, we calculate $E \sim 22$ kcal mol⁻¹. However, this is probably too high, since the hydroperoxide was not observed as a product in the study of Niki et al.,¹³ which was carried out at atmospheric pressure in the gas phase. It is more reasonable to estimate a half-life of about 1 s or less, which leads to $E^* = 17$ kcal mol⁻¹. This is used in Figure 3.

If hydroxyacetone is formed by isomerization of the hydroperoxide, then we need to consider its further possible reactions since it will be formed with a large amount of excess energy. We consider two possible subsequent reactions: a simple bond breaking to yield radical products and a complex molecular elimination to yield the observed product, methylglyoxal. On the basis of the computer simulation, we set k_B (bond breaking) = 10 k_E (elimination). For the bond-breaking reactions, we estimate, by analogy with data on acetone pyrolysis,²⁶ that $A_9 = 10^{16.3}$ s⁻¹. The activation energy is taken to be the heat of reaction, i.e., $E_9^* = 76$ kcal mol⁻¹. The total energy is $E = 126$ kcal mol⁻¹, and

$$k_9 = 10^{16.3} \left\{ \frac{126 - 76}{126} \right\}^{s-1} \text{ s}^{-1}$$

To estimate s from the expression $s_{\text{eff}} = (C_p - 8)/R$, we again evaluate the temperature for which

$$\int_0^T (C_p - 8) dt = 50000 \text{ cal mol}^{-1}$$

where 50000 cal mol⁻¹ is E^{**} , the thermal energy of the "hot" hydroxyacetone. The temperature obtained is $T \sim 2000$ K for which $C_p \approx 51$ cal mol⁻¹ K⁻¹. Hence $s_{\text{eff}} = (C_p - 8)/R = 21.5$. Therefore

$$k_9 = 10^{16.3} \left\{ \frac{126 - 76}{126} \right\}^{20.5} = 10^{8.1} \text{ s}^{-1}$$

and $k_{10} = 0.1k_9 = 10^{7.1} = 10^{12} \{126 - E^*/126\}^{20.5}$ s⁻¹. Here we have chosen the A factor on the basis of the observed A factors for hydrogen halide and water elimination reactions.²⁶ The calculated activation energy for the elimination reaction is then $E_{10}^* = 53$ kcal mol⁻¹.

Again we can compare the calculated rate constants, $k_9 = 10^{8.1}$ and $k_{10} = 10^{7.1}$ s⁻¹, with the collision rate of 10^{7.1} s⁻¹. Fortuitously, this indicates that quenching to form stabilized hydroxyacetone is about as important as the formation of methylglyoxal in the H₂ elimination reaction, as observed.

Conclusions

The computer simulation of our experimental results suggests that the ester channel is not operative for Me₂COO from O₃ + TME. That is, subsequent to its formation, there is a significant change in the mechanistic path followed by a Criegee intermediate R'R''COO depending on the nature of R' and R'': for R' = R'' = H, it appears to follow the ester channel; for R' ≠ H and/or

(25) Batt, L.; Liu, M. T. H. "Pyrolysis of Peroxides in the Gas Phase", In *The Chemistry of Functional Groups, Peroxides*; Patai, S., Ed.; Wiley: New York, 1983.

(26) Benson, S. W.; O'Neal, H. E. *Kinetic Data on Gas Phase Unimolecular Reactions*, U.S. Government Printing Office: Washington, D.C. 20402, 1970; NSRDS-NBS 21.

(27) Nangia, P. S.; Benson, S. W. *Int. J. Chem. Kinet.* **1980**, *12*, 43.

(28) Nangia, P. S.; Benson, S. W. *J. Phys. Chem.* **1979**, *83*, 1138.

$R'' \neq H$, the ester channel apparently cannot compete with the hydroperoxide channel. Our modeling studies suggest this may be true for TME and possibly also for isobutene, propene, and 2-butene. If correct, then atmospheric models will have to be modified to account for this significantly greater reactivity in ozonolysis reactions.

The secondary reactions included in the computer model can account for the stoichiometry observed in the gas-phase $O_3 + TME$

reaction. This reaction appears to proceed through the hydroperoxide and hydroxyacetone, as it does in solution. Moreover, the computer simulation and the zeroth-order thermochemical kinetics estimates suggest that hydroxyacetone and methylglyoxal are both "prompt" products resulting from sequential isomerizations subsequent to the formation of the Me_2COO .

Registry No. TME, 563-79-1.

Pulse Radiolytic Investigations of Aqueous Solutions of Methoxybenzene Cation Radicals: The Effect of Colloidal RuO_2

Marek Brandys,[†] Richard E. Sassoon,[‡] and Joseph Rabani*

Energy Research Center and The Department of Physical Chemistry, The Hebrew University of Jerusalem, Jerusalem 91904, Israel (Received: August 1, 1985; In Final Form: September 11, 1986)

The formation and decay of the radical cations of 1,4-dimethoxybenzene (DMB) and 1,2,4,5-tetramethoxybenzene (TMB) were investigated by the pulse radiolysis technique in the absence and the presence of colloidal RuO_2 particles. $DMB^{+\bullet}$ was obtained only by Tl^{2+} oxidation of DMB while $TMB^{+\bullet}$ was produced by oxidation of TMB using both Tl^{2+} and Br_2^- . In the absence of RuO_2 both $DMB^{+\bullet}$ and $TMB^{+\bullet}$ decay predominantly via a second-order process, although there is a contribution of a pseudo-first-order reaction. The rate constants for these reactions are reported. RuO_2 colloidal particles catalyze the decay of both $TMB^{+\bullet}$ and $DMB^{+\bullet}$. The reactions of $TMB^{+\bullet}$ with RuO_2 were found to depend on pH, pulse intensity, and colloid concentration. At pH 3-4, adsorption of $TMB^{+\bullet}$ to the colloid is observed, followed by the decay of the remaining $TMB^{+\bullet}$ in the bulk. At higher pHs, loading of the RuO_2 colloid by positive holes takes place until equilibrium is achieved between loaded holes and $TMB^{+\bullet}$ and again the remaining $TMB^{+\bullet}$ decays at a later stage. The fraction of $TMB^{+\bullet}$ that loads the colloidal particles increases with both pH and $[RuO_2]$. It is also suggested that $DMB^{+\bullet}$ loads the RuO_2 at the pH where experiments were performed. $(TMB)_2$ and $(DMB)_2$ dimers (or higher oligomers) are suggested to be the final products both in the absence and presence of RuO_2 . No O_2 is formed with the RuO_2 colloid despite a favorable redox potential for water oxidation.

Introduction

Alkoxybenzenes are known to be good electron donors and may serve as quenchers in photoinduced electron-transfer systems.¹ For example 1,4-dimethoxybenzene (DMB) and 1,2,4,5-tetramethoxybenzene (TMB) possess many ideal properties that may make them suitable as positive hole relays in catalytic light-energy conversion systems. They have high positive redox potentials ($E^\circ_{DMB^{+\bullet}/0} = 1.59$ V, $E^\circ_{TMB^{+\bullet}/0} = 1.06$ V vs. NHE²) and relatively high solubilities in water (slightly less than 10^{-2} M) and produce relatively stable cation radicals.³⁻⁵ Both have been shown to quench various photosensitizers such as acridine orange,⁶ $Ir(bpy)_2(Hbpy-C^3, N^7)^{3+}$,⁷ and UO_2^{2+} ⁸ at nearly diffusion-controlled rates. Several methoxybenzenes have also been found to quench a polypyridylruthenium derivative as a photosensitizer.⁹ It was shown that in acetonitrile oxidative quenching takes place with rates 2-3 orders of magnitude slower than those that are diffusion controlled. The lifetimes of the photochemical products are, however, relatively short.

The methoxybenzenes used in this work were therefore considered to be very suitable as model systems for oxidizing relays in which they can transfer positive charge either to an appropriate catalyst or to an added donor species in solution. Several investigations³⁻⁵ have already been carried out in order to study the nature of the methoxy radical cations, and hence the aim of our work is to fully understand the nature of oxidized DMB and TMB radicals by using the pulse radiolytic technique and to investigate their decay in the presence of a colloidal RuO_2 catalyst in order to probe the role of RuO_2 as a catalyst for water oxidation.

Experimental Section

Materials. 1,4-Dimethoxybenzene (Aldrich) was recrystallized once from methanol, and 1,2,4,5-tetramethoxybenzene was prepared with minor modifications according to the literature method¹⁰ and gave good microanalysis results after threefold recrystallization from water. Since tetramethoxybenzene solutions were found to decompose during prolonged storage of more than several days, as indicated by changes in their absorption spectra, only freshly prepared solutions were used. The cation radicals were generated by the pulse radiolysis technique in N_2O -saturated solutions containing either Tl_2SO_4 (BDH) or NaBr (Baker analyzed). Buffers consisted of standard pH control solutions.¹¹ All other reagents were of the highest purity available and were used without further treatment while water was distilled and passed

(1) Ballardini, R.; Varani, G.; Balzani, V. *J. Am. Chem. Soc.* **1980**, *102*, 1719.

(2) Mann, C. K.; Barnes, K. K. *Electrochemical Reactions in Non-Aqueous Systems*, Marcel Dekker: New York, 1970.

(3) O'Neill, P.; Steenken, S.; Schulte-Frohlinde, D. *Angew. Chem., Int. Ed. Engl.* **1975**, *14*, 430.

(4) O'Neill, P.; Steenken, S.; Schulte-Frohlinde, D. *J. Phys. Chem.* **1975**, *79*, 2773.

(5) Sullivan, P. D.; Brelte, N. A. *J. Phys. Chem.* **1975**, *79*, 474.

(6) Vogelmann, E.; Rauscher, W.; Kramer, H. E. A. *Photochem. Photobiol.* **1979**, *29*, 771.

(7) Slama-Schwok, A.; Rabani, J., to be published.

(8) Brandeis, M.; Sassoon, R. E.; Rabani, J. *Int. Conf. Photochem. Convers. Storage Solar Energy, 5th*, **1984**, Paper A76(1).

(9) Monserrat, K.; Foreman, T. K.; Graetzel, M.; Whitten, D. G. *J. Am. Chem. Soc.* **1981**, *103*, 6667.

(10) (a) Benington, F.; Morin, R. D.; Clark, L. C. *J. Org. Chem.* **1955**, *20*, 102. (b) Veda, M.; Sakai, N.; Imai, Y. *Makromol. Chem.* **1979**, *180*, 2813.

(11) Dean, J. A., Ed. *Lange's Handbook of Chemistry*, McGraw Hill: New York, 1979; Tables 5-23, pp 5.77-5.78.

[†] Present address: Vitreous State Laboratory, Keane Hall, The Catholic University of America, Washington, D.C. 20064.

[‡] Present address: Radiation Laboratory, University of Notre Dame, Notre Dame, Indiana 46556.